Chen et al. Nanoscale Research Letters (2017) 12:238
DOI 10.1186/s11671-017-1992-1

Nanoscale Research Letters

NANO EXPRESS

Open Access

Enhanced Performance of Planar Perovskite Solar Cells Using Low-Temperature Solution-Processed Al-Doped SnO_2 as Electron Transport Layers

Hao Chen[1], Detao Liu[1], Yafei Wang[1], Chenyun Wang[1], Ting Zhang[1], Peng Zhang[1], Hojjatollah Sarvari[2], Zhi Chen[2*] and Shibin Li[1*]

Abstract

Lead halide perovskite solar cells (PSCs) appear to be the ideal future candidate for photovoltaic applications owing to the rapid development in recent years. The electron transport layers (ETLs) prepared by low-temperature process are essential for widespread implementation and large-scale commercialization of PSCs. Here, we report an effective approach for producing planar PSCs with Al^{3+} doped SnO_2 ETLs prepared by using a low-temperature solution-processed method. The Al dopant in SnO_2 enhanced the charge transport behavior of planar PSCs and increased the current density of the devices, compared with the undoped SnO_2 ETLs. Moreover, the enhanced electrical property also improved the fill factors (FF) and power conversion efficiency (PCE) of the solar cells. This study has indicated that the low-temperature solution-processed Al-SnO_2 is a promising ETL for commercialization of planar PSCs.

Keywords: Perovskite solar cells, Electron transport layers, Low-temperature solution-process, Al-doped SnO_2

Background

The solar energy has attracted much attention since it is a renewable and clean energy source [1–4]. In recent years, a large amount of research groups have focused on organic-inorganic lead halide perovskite solar cells as it have the advantages of a lower manufacturing cost and a simpler process compared with Si solar cells. Moreover, PSCs have a great potential for providing an alternative to conventional photovoltaic devices. The PCE of PSCs has increased from 3.8 to 22.1% in a few years [5–9]. However, the efficiency and stability of PSCs strongly depend on some crucial factors, for instance, the morphology of perovskite films and the preparation of electron/hole transport material [10–15].

Both electron transport layers (ETLs) and hole transport layers (HTLs), which can extract electrons and holes from the light harvesting layers, respectively, are essential for the high-efficiency PSCs. Most of the high performance, PSCs were accomplished using compact TiO_2 layer or mesoporous TiO_2 layer as the ETLs [8, 16]. However, the processes of both the compact TiO_2 layer and the mesoporous TiO_2 layer generally require a high sintering temperature (>450 °C), which is an obstacle for the stretchable device fabrication and the commercial development of PSCs [17, 18]. Previously, SnO_2 has shown up as an effective electron transport layer in perovskite solar cells due to the wider band gap (about 3.6 eV) and higher mobility (100 to 200 $cm^2V^{-1}s^{-1}$) compared with TiO_2 [19–21]. Furthermore, the temperature of forming SnO_2 thin films (<200 °C) is helpful for widespread implementation and large-scale commercialization of PSCs [22]. Therefore, SnO_2 is a promising candidate for ETLs used in high-performance PSCs.

It has been reported that doping ETLs with metal aliovalent cations are an effective method to improve properties of both ETLs and ETLs/perovskite interfaces. Other groups have already doped Y^{3+} and Li^+ in SnO_2 to improve carrier transport and optical abilities

* Correspondence: zhichen@engr.uky.edu; shibinli@uestc.edu.cn
[2]Department of Electrical and Computer Engineering, Center for Nanoscale Science and Engineering, University of Kentucky, Lexington, KY 40506, USA
[1]State Key Laboratory of Electronic Thin Films and Integrated Devices, School of Optoelectronic Information, University of Electronic Science and Technology of China (UESTC), Chengdu, Sichuan 610054, China

[23, 24]. In addition, doping can also improve the conductivity of ETLs and optimize the energy level matching between ETLs and the perovskite film, resulting in the enhanced performance of device [23].

Here, we present a low-temperature synthesized Al-doped SnO_2 as an ETL in the n-i-p structure perovskite solar cells. Al-doped SnO_2 thin films prepared at a low temperature (190 °C) show a better charge transport and electron extraction behavior than the pristine SnO_2. The enhanced electrical property of SnO_2 improves the PCE, V_{OC}, J_{SC}, and fill factor (FF) of the PSCs. The champion cell based on Al-doped SnO_2 reaches a PCE of 12.10% with a V_{OC} of 1.03 V, a J_{SC} of 19.4 mA/cm^2, and a FF of 58%, while the PSCs based on undoped SnO_2 achieves a PCE of 9.02% with a V_{OC} of 1.00 V, a J_{SC} of 16.8 mA/cm^2, and a FF of 53%.

Methods

The fluorine-doped tin oxide (FTO) glass substrates were sequentially cleaned with acetone, ethyl alcohol, and deionized (DI) water in the ultrasonic bath for 15 min. Then the substrates were dried by a N_2 flow and further cleaned by UV-ozone for 10 min before the deposition of SnO_2.

SnO_2 and Al-SnO_2 ETLs were deposited by a spin-coating method. The solution was prepared by dissolving $SnCl_4{\bullet}5H_2O$ in isopropyl alcohol at a concentration of 0.075 M and subsequently stirred for 60 min at room temperature. For Al-doping, we dissolved $AlCl_3{\bullet}6H_2O$ in isopropyl alcohol. Then this aluminum precursor was added to the antecedent solution at a series of molar ratio and stirred until the solution became clear. Afterwards, the two different kinds of solution were separately deposited on cleaned FTO substrates at 3000 rpm for 30 s. The substrates were then pre-dried at 100 °C for 10 min and annealed at 190 °C for 1 h.

After the deposition of SnO_2 and Al-SnO_2 electron transport layers, the samples were treated by UV-ozone for 10 min again. The $CH_3NH_3PbI_3$ film was fabricated by a one-step spin-coating method. The $CH_3NH_3PbI_3$ solution (45 wt%) was deposited on the treated SnO_2 at 5000 rpm for 30 s. 0.5 mL chlorobenzene was dropped onto the substrate when spin-coating the $CH_3NH_3PbI_3$ solution. All the perovskite layers were annealed at 100 °C for 10 min. The hole transport layers were deposited by spin-coating the 2,29,7,79-tetrakis(N,Ndi-p-methoxyphenylamine)-9,9-spirobifluorene (spiro-OMeTAD) solution at 4000 rpm for 30 s. Finally, 100-nm-thick gold top electrode was deposited on the HTL via thermal evaporation.

Device Characterization

The J-V characteristics of perovskite solar cells were measured by Keithley 2400 source measuring unit under the AM 1.5 G solar-simulated light (Newport Oriel Solar 3 A Class AAA, 64023 A). The sun light (100 mw/cm^2) was calibrated by a standard Si-solar cell (Oriel, VLSI standards). X-ray photoelectron spectroscopy (XPS) was measured using the Kratos XSAM 800 X-Ray Photoelectron Spectrometer.

Result and Discussion

In our work, SnO_2 layers have been deposited on FTO substrates by a low-temperature solution method. Top view scanning electron micrographs (SEM) of the SnO_2 and bare FTO are shown in Fig. 1a–b. A dense and pinhole-free film is formed by spin coating SnO_2 ETLs solution on FTO substrates, suggesting that the FTO substrates have been fully covered. Dense ETLs are known as an essential element of high-performance PSCs. Thus, a compact SnO_2 layer deposited on FTO can enhance the interfacial contact with perovskite layers and improve the performance of the solar cells [25].

To examine the efficiency of PSCs based on the low-temperature solution-processed SnO_2 and Al-SnO_2 ETLs, we have fabricated the planar solar cells with the structure of FTO/(Al-)SnO_2/$MAPbI_3$/Spiro-OMeTAD/Au shown in Fig. 1d. In addition, Fig. 1c shows a cross-sectional SEM image of a PSC based on Al-doped SnO_2 layer without the Au electrode, and the energy band diagram of PSCs is shown in Fig. 1e.

To confirm that the employment of Al-doping SnO_2 as ETLs has no effect on the perovskite films, we measured the UV-vis absorbance spectra and the corresponding X-ray diffraction (XRD) of the $MAPbI_3$ film on FTO/SnO_2 and FTO/Al-SnO_2 substrates. The results are shown in Fig. 2a and b, respectively. The $MAPbI_3$ films deposited on SnO_2 and Al-SnO_2 ETLs exhibit almost identical absorbance spectra, suggesting that the absorption of the perovskite films is nearly not affected by Al-doping in SnO_2 ETLs.

As to the XRD patterns, several strong peaks are located at 14.05, 23.44, 24.25, 28.18, 31.88, 34.93, and 40.16°. All these peaks can be assigned to orthorhombic crystal of the perovskite with high crystallization [26–28]. The XRD patterns show negligible difference between the samples of FTO/SnO_2/$MAPbI_3$ and FTO/Al-SnO_2/$MAPbI_3$, indicating the dopant of Al in SnO_2 film does not affect on the structure property of $MAPbI_3$ film. Furthermore, the main PbI_2 peak is absent from the XRD patterns, which indicates PbI_2 has sufficiently reacted with MAI.

As the evidences were obtained from the UV-vis absorbance spectra and XRD patterns of the devices, the dopant of Al in SnO_2 does not cause any obvious changes on the structure and optical properties in the perovskite layers. Therefore, the performance enhancement induced by Al-doping in SnO_2 as ETLs is most likely due to the improvement of the ETLs/perovskite

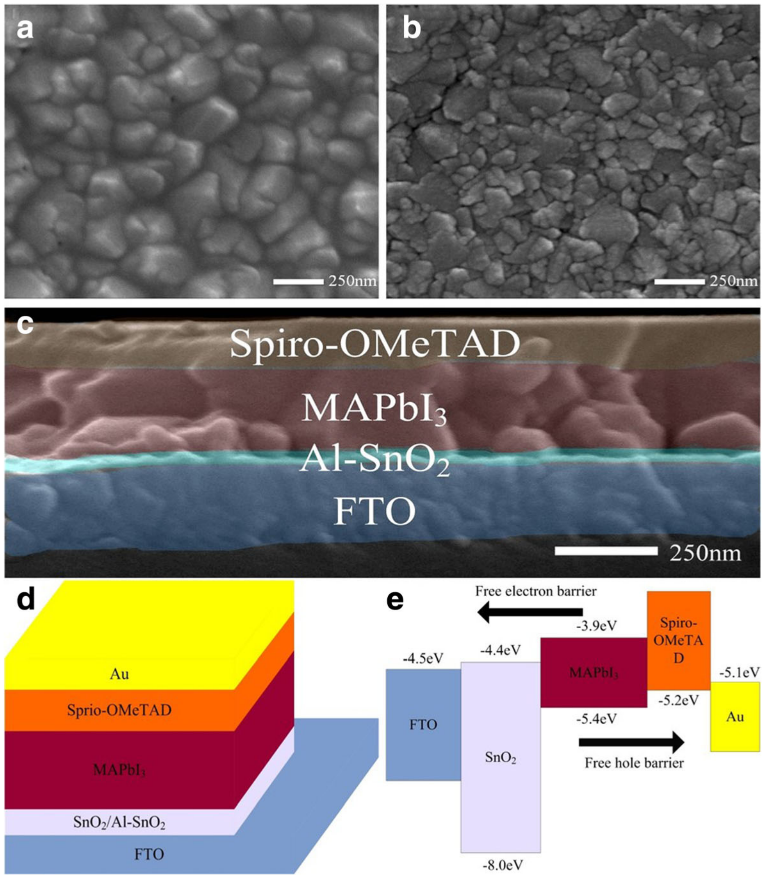

Fig. 1 **a** Top view SEM images of low-temperature solution-processed SnO_2 on FTO and **b** bare FTO. **c** Cross-sectional SEM image of the planar perovskite solar cell based on Al-SnO_2, **d** schematic of the PSCs grown on Al-SnO_2, and **e** energy band diagram of the PSCs

interfacial properties. In other words, the charge transport and electron extraction are improved.

Figure 2c illustrates the external quantum efficiency (EQE) spectrum of the best-performance solar cells based on SnO_2 and Al-SnO_2. Obviously, the EQE of Al-doped device is higher than the device based on pristine SnO_2 over the entire wavelength range. The higher EQE means superior electron extraction capability of the ETLs [29]. The calculated J_{SC} (≈19.0 mA/cm^2) based on Al-SnO_2 from the EQE spectra is consistent with the measured value of the current density-voltage (J-V) curves measured under the one-sun light. As for undoped SnO_2, the calculated J_{SC} is approximately equal to 16.6 mA/cm^2.

The J-V curves of the best-performance PSCs based on SnO_2 and Al-SnO_2 ETLs are shown in Fig. 2d. The PCE increases from 9.02 to 12.10% by doping SnO_2 with Al. Al-doping may cause an improvement on the charge transport and electron extraction behavior of the SnO_2, leading to the increment of the J_{SC} (16.8 to 19.4 mA/cm^2). Furthermore, the V_{OC} of the best PSC based on Al-SnO_2 (1.03 V) is a little higher than that of the best cell based on SnO_2 (1.00 V), indicating less energy loss of electrons [30]. Therefore, the enhanced parameters mentioned above leads to the improvement of FF (53 to 58%).

Al-SnO_2 films deposited by a low-temperature solution-processed were further investigated by X-ray photoemission spectroscopy (XPS). Figure 3a displays the full XPS spectrum, which shows the presence of O, C, and Sn. The binding energies of 487.3 and 495.8 eV shown in Fig. 3b corresponds to Sn $3d_{5/2}$ and Sn $3d_{3/2}$, respectively. The main binding energy of 531.0 eV shown in Fig. 3c corresponds to O 1 s, which reveals the O^{2-} state in SnO_2 [21]. The absence of Al in the full XPS spectrum can be attributed to the low concentration (5% molar ratio), while Al 2p peak can be observed in Fig. 3d with a relatively low content, indicating that the doping is truly practicable. Identically, the Cl 2p peak missed in the full XPS spectrum can also be observed in Fig. 2e. The low-content Cl suggests that both most of $SnCl_4$ and $AlCl_3$ have been oxidized.

To identify the reasons for the enhanced performance due to the Al-doping, we carried out the time-resolved photoluminescence (TRPL) to study the electron-extraction

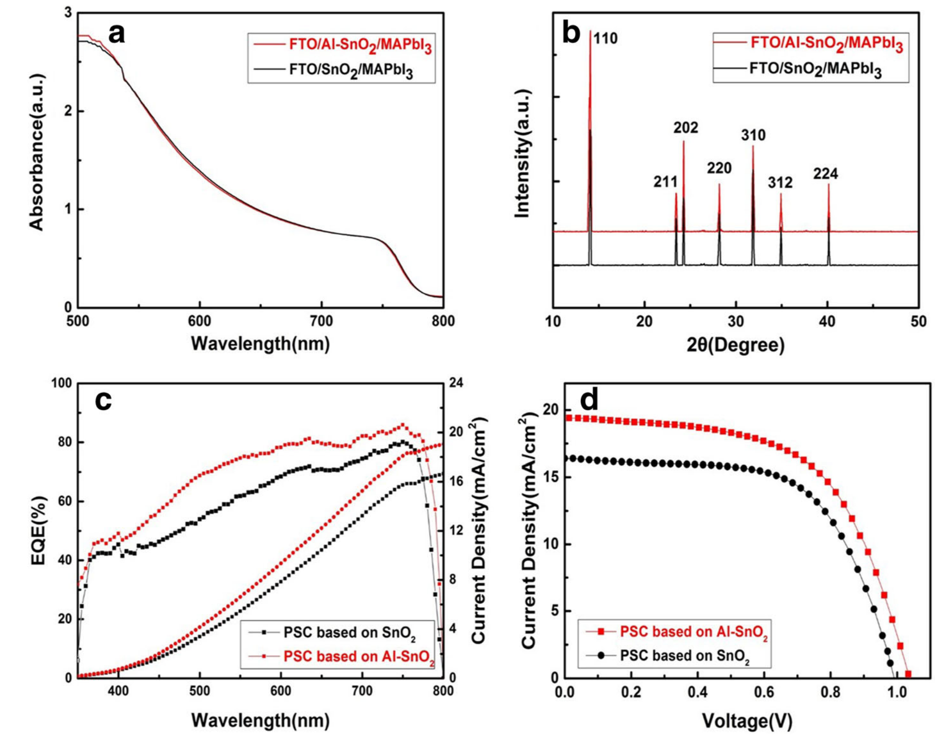

Fig. 2 **a** UV-vis absorbance spectra and **b** XRD patterns of perovskite films grown on SnO2 and Al-SnO2 substrates. **c** EQE curves and integrated current density of perovskite solar cells based on SnO2/Al-SnO2 and **d** J-V curves of the best-performing PSC using SnO2/Al-SnO2 ETLs

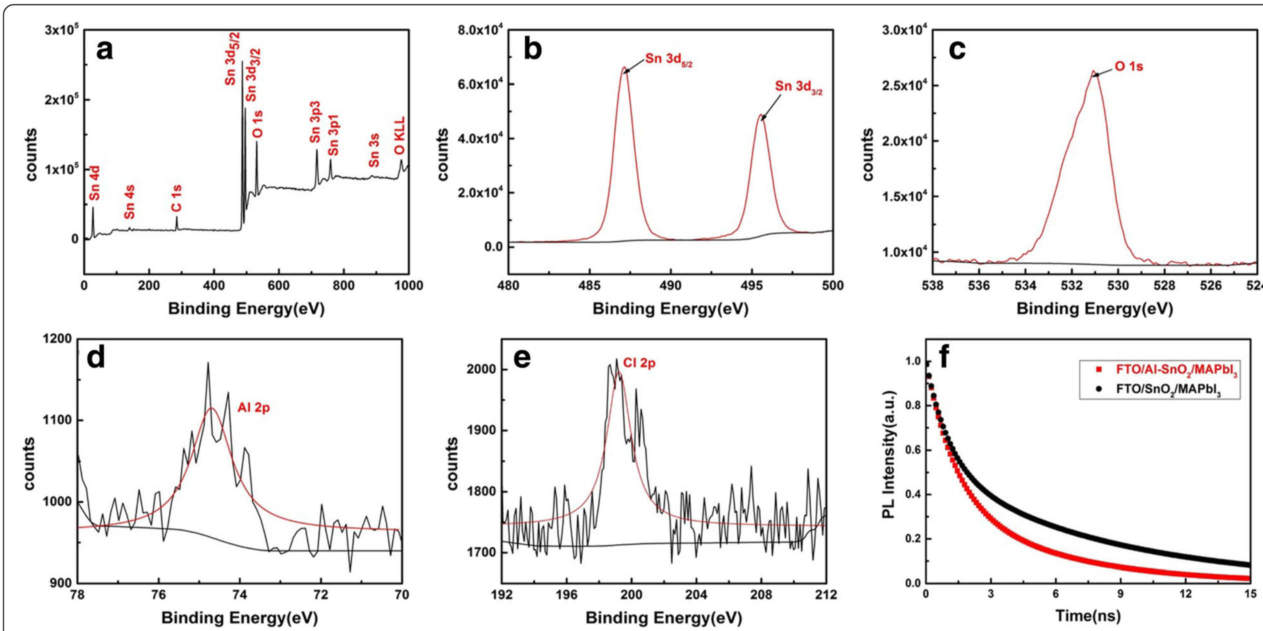

Fig. 3 XPS spectra of **a** survey, **b** Sn 3d, **c** O 1 s, **d** Al 2p, and **e** Cl 2p peaks for Al-SnO_2 film deposited on the FTO substrate. **f** Normalized time-resolved PL decay curves of $MAPbI_3$ films deposited on SnO_2 (*black line*) and Al-SnO_2 (*red line*) coated substrates

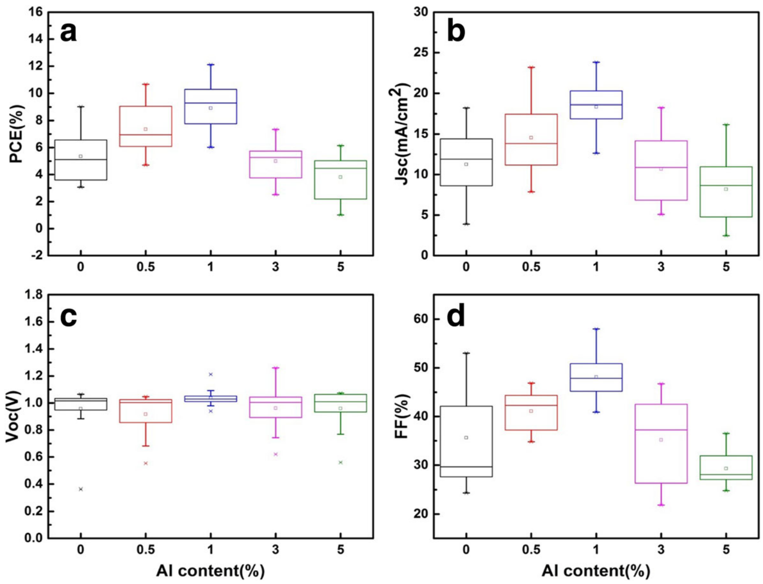

Fig. 4 Histograms of the different Al content on photovoltaic parameters including **a** PCE, **b** J_{SC}, **c** V_{OC}, and **d** FF

behavior of different ETLs. The TRPL decay curves, shown in Fig. 3f, are exponentially fitted, where τ1and τ2 represent the bulk recombination in perovskite bulk films and the delayed recombination of trapped charges, respectively [31]. For the FTO/SnO_2/$MAPbI_3$ sample, τ1 is 1.07 ns and τ2 is 7.98 ns, while τ1 is 1.32 ns and τ2 is 5.13 ns for the doped SnO_2 sample (1% Al-doping content). Apparently, the perovskite film deposited on the Al-SnO_2 ETL has a lower τ2 with a lower ratio of τ2/τ1, indicating a better change transfer from perovskite to ETLs and more efficient extraction of the photo-induced electrons between the perovskite and ETLs, as compared to the film deposited on the pristine SnO_2 ETL [32, 33]. In addition, the decay curves also confirm the remarkable enhancement of the electron extraction and charge transport induced by Al-doping in SnO_2. These properties result in the improvement of current density and the power conversion efficiency.

We also compared four different parameters of the cell performance with a series of doping concentration. From the box charts in Fig. 4a, it is obvious that the PCE of the cells is strongly influenced by Al doping. The average PCE of the cells is improved with the increment of Al content before the concentration of 1%, while the average PCE is reduced with the higher Al content (3 and 5%). The change of J_{SC} of these solar cells is shown in Fig. 4b, and the variation tendency is like the trend of PCE. The highest J_{SC} is 23.82 mA/cm^2, which confirms a good charge transportation of the cells. Regarding the change of V_{OC}, Fig. 4c shows the variation of V_{OC}, value is smallest with 1% Al-doping content. The results demonstrate that the solar cells with 1% Al-doping exhibit the best repeatability. As exhibited in Fig. 4d, the change tendency of FF is analogous to the trend of PCE. In addition, the average FF of the solar cells doped with 0.5 and 1% Al^{3+} content is higher than the undoped solar cells impressively. The results mentioned above reveal that a suitable Al-doping is beneficial for the performance of the perovskite solar cells based on SnO_2.

Conclusions

In summary, we studied the effect of Al-doping on SnO_2 as ETLs for planar perovskite solar cells. According to the results of UV-vis absorbance spectra and XRD patterns of perovskite films deposited on Al-SnO_2 and SnO_2, the Al dopant in SnO_2 does not influence the structure and optical properties of the perovskite layers. Based on the TRPL test, the Al-dopant in SnO_2 enhances the charge transport and electron extraction behavior of the PSCs and then the J_{SC} of the devices is improved. The champion cell based on Al-SnO_2 exhibited a higher efficiency of 12.10% than that using SnO_2 (9.02%) as ETLs. Our results suggest that efficient planar perovskite solar cells based on SnO_2 can be fabricated by doping SnO_2 with Al^{3+}.

Funding

This work was supported by the National Natural Science Foundation of China under grant nos. 61421002, 61574029, and 61371046. This work was also partially supported by University of Kentucky.

Authors' Contributions

HZ, DL, and FW designed and carried out the experiments. CW, TZ, PZ, and HS participated in the work to analyze the data and prepared the manuscript initially. SL and ZC gave equipment support. All authors read and approved the final manuscript.

Competing Interests

The authors declare that they have no competing interests.

Publisher's Note

Springer Nature remains neutral with regard to jurisdictional claims in published maps and institutional affiliations.

Received: 21 February 2017 Accepted: 10 March 2017
Published online: 31 March 2017

References

1. Grätzel M (2005) Solar energy conversion by dye-sensitized photovoltaic cells. Inorg Chem 44(20):6841–6851
2. Zheng Y, Goh T, Fan P et al (2016) Toward efficient thick active PTB7 photovoltaic layers using diphenyl ether as a solvent additive. ACS Appl Mat Interfaces 8(24):15724–15731
3. Goswami DY, Vijayaraghavan S, Lu S et al (2004) New and emerging developments in solar energy. Sol Energy 76(1):33–43
4. Xing S, Wang H, Zheng Y et al (2016) Förster resonance energy transfer and energy cascade with a favorable small molecule in ternary polymer solar cells. Sol Energy 139:221–227
5. Kojima A, Teshima K, Shirai Y et al (2009) Organometal halide perovskites as visible-light sensitizers for photovoltaic cells. J Am Chem Soc 131(17):6050–6051
6. Zhang ZL, Li JF, Wang XL et al (2017) Enhancement of perovskite solar cells efficiency using N-doped TiO_2 nanorod arrays as electron transfer layer. Nanoscale Res Lett 12(1):43
7. Li S, Zhang P, Chen H et al (2017) Mesoporous PbI_2 assisted growth of large perovskite grains for efficient perovskite solar cells based on ZnO nanorods. J Power Sources 342:990–997
8. Wang Y, Li S, Zhang P et al (2016) Solvent annealing of PbI_2 for the high-quality crystallization of perovskite films for solar cells with efficiencies exceeding 18%. Nanoscale 8(47):19654–19661
9. NREL: National Center For Photovoltaics Home Page. https://www.nrel.gov/pv(2016). Accessed 30 July 2016.
10. Yang WS, Noh JH, Jeon NJ et al (2015) High-performance photovoltaic perovskite layers fabricated through intramolecular exchange. Science 348(6240):1234–1237
11. Li S, Zhang P, Wang Y et al (2016) Nano Res. doi:10.1007/s12274-016-1407-0
12. Saliba M, Matsui T, Seo JY et al (2016) Cesium-containing triple cation perovskite solar cells: improved stability, reproducibility and high efficiency. Energy Environ Sci 9(6):1989–1997
13. Liu M, Johnston MB, Snaith HJ (2013) Efficient planar heterojunction perovskite solar cells by vapour deposition. Nature 501(7467):395–398
14. Chen LC, Chen JC, Chen CC et al (2015) Fabrication and properties of high-efficiency perovskite/PCBM organic solar cells. Nanoscale Res Lett 10(1):312
15. Li H, Li S, Wang Y et al (2016) A modified sequential deposition method for fabrication of perovskite solar cells. Sol Energy 126:243–251
16. Wang W et al (2016) Enhanced performance of $CH_3NH_3PbI_{3-x}Cl_x$ perovskite solar cells by CH_3NH_3I modification of TiO_2-perovskite layer interface. Nanoscale Res Lett. doi:10.1186/s11671-016-1540-4
17. Kim HS et al (2012) Lead iodide perovskite sensitized all-solid-state submicron thin film mesoscopic solar cell with efficiency exceeding 9%. Sci Rep 2:591
18. Jeon NJ, Noh JH, Kim YC et al (2014) Solvent engineering for high-performance inorganic–organic hybrid perovskite solar cells. Nat Mater 13(9):897–903
19. Jiang Q, Zhang L, Wang H et al (2016) Enhanced electron extraction using SnO_2 for high-efficiency planar-structure $HC(NH_2)_2PbI_3$-based perovskite solar cells. Nat Energy 1:16177
20. Chandiran AK, Abdi-Jalebi M, Nazeeruddin MK et al (2014) Analysis of electron transfer properties of ZnO and TiO_2 photoanodes for dye-sensitized solar cells. ACS Nano 8(3):2261–2268
21. Ke W, Fang G, Liu Q et al (2015) Low-temperature solution-processed tin oxide as an alternative electron transporting layer for efficient perovskite solar cells. J Am Chem Soc 137(21):6730–6733
22. Anaraki EH, Kermanpur A, Steier L et al (2016) Highly efficient and stable planar perovskite solar cells by solution-processed tin oxide. Energ Environ Sci 9(10):3128–3134
23. Yang G, Lei H, Tao H et al (2017) Reducing hysteresis and enhancing performance of perovskite solar cells using low-temperature processed Y-doped SnO_2 nanosheets as electron selective layers. Small. doi:10.1002/smll.201601769
24. Park M, Kim JY, Son HJ et al (2016) Low-temperature solution-processed Li-doped SnO_2 as an effective electron transporting layer for high-performance flexible and wearable perovskite solar cells. Nano Energy 26:208–215
25. Xiong L, Qin M, Yang G et al (2016) Performance enhancement of high temperature SnO_2-based planar perovskite solar cells: electrical characterization and understanding of the mechanism. J Mater Chem A 4(21):8374–8383
26. Im JH, Lee CR, Lee JW et al (2011) 6.5% efficient perovskite quantum-dot-sensitized solar cell. Nanoscale 3(10):4088–4093
27. Baikie T, Fang Y, Kadro JM et al (2013) Synthesis and crystal chemistry of the hybrid perovskite $(CH_3NH_3)PbI_3$ for solid-state sensitised solar cell applications. J Mater Chem A 1(18):5628–5641
28. Stoumpos CC, Malliakas CD, Kanatzidis MG (2013) Semiconducting tin and lead iodide perovskites with organic cations: phase transitions, high mobilities, and near-infrared photoluminescent properties. Inorg Chem 52(15):9019–9038
29. Agresti A, Pescetelli S, Cinà L et al (2016) Efficiency and stability enhancement in perovskite solar cells by inserting lithium-neutralized graphene oxide as electron transporting layer. Adv Funct Mater 26:2686–2694
30. Liu D, Li S, Zhang P et al (2017) Efficient planar heterojunction perovskite solar cells with Li-doped compact TiO_2 layer. Nano Energy 31:462–468
31. Li Y, Zhao Y, Chen Q et al (2015) Multifunctional fullerene derivative for interface engineering in perovskite solar cells. J Am Chem Soc 137(49):15540–15547
32. Ke W, Zhao D, Xiao C, Wang C et al (2016) Cooperative tin oxide fullerene electron selective layers for high-performance planar perovskite solar cells. J Mater Chem A 4(37):14276–14283
33. Chen W, Wu Y, Yue Y et al (2015) Efficient and stable large-area perovskite solar cells with inorganic charge extraction layers. Science 350(6263):944–948